Life Sciences 218 (2019) 241–252

Contents lists available at ScienceDirect

Life Sciences

journal homepage: www.elsevier.com/locate/lifescie

Dynamic decreased expression and hypermethylation of secreted frizzled-related protein 1 and 4 over the course of pulmonary fibrosis in mice

Junfei Zhou[a], Zheng Yi[a,*], Qiang Fu[b]

[a] Department of Rheumatology, Beijing Chao-Yang Hospital, Capital Medical University, Beijing 100020, PR China
[b] Department of Rheumatology, The First Affiliated Hospital of University of South China, HengYang 421001, PR China

ARTICLE INFO

Keywords:
Secreted frizzled-related protein
Hypermethylation
Pulmonary fibrosis
Bleomycin
Mice

ABSTRACT

Aberrantly activated Wnt signaling pathway and dysregulation of extracellular antagonists of Wnt signaling have been revealed in pulmonary fibrosis. In this study we evaluated the expression of secreted frizzled-related proteins (SFRPs) and their aberrant promoter methylation to investigate the involvement of epigenetic regulation in pulmonary fibrosis. The pulmonary fibrosis induced by intratracheal injection of bleomycin (BLM) into mice was adopted. The transcription and relative protein expression of SFRPs were detected at Day 7 (D7), D14, and D21. DNA methylation analysis was performed by methylation-specific polymerase chain reaction (MSP). A DNA methyltransferase (DNMT) inhibitor (5-aza-2′-deoxycytidine; 5-aza) was used for demethylation and the relative β-catenin expression levels were measured to assess overactivity of the canonical Wnt signaling pathway. The transcription and protein expression of SFRP1 significantly decreased at D14 and D21, whereas the transcription and protein expression of SFRP4 significantly decreased at D7 and stayed downregulated until D21. The significantly hypermethylated promoters of SFRP1 and SFRP4 resulted in impaired transcription and decreased expression during pulmonary fibrosis in mice. Besides, reactivation of SFRP1 and SFRP4 by 5-aza reduced β-catenin mRNA and protein expression *in vivo* and *in vitro*. Animal experiments confirmed that 5-aza could significantly alleviate bleomycin-induced pulmonary fibrosis in mice. Thus, changes of promoter hypermethylation might downregulate SFRP1 and SFRP4 at different stages of pulmonary fibrosis, and the finding supports the usefulness of DNMT inhibitors, which might effectively reverse activation of β-catenin and reduce pulmonary fibrosis in mice. These data provide a possible new direction in the research on pulmonary fibrosis treatments.

1. Introduction

Pulmonary fibrosis is a chronic, progressive and fatal disease. Although the etiology is still unclear, some commonly used drugs and special environmental factors, and even abnormal regulation of immunity (*i.e.*, autoimmunity) may be responsible [1]. The pathophysiological characteristics include the following: infiltrating inflammatory cells are observed at the early stage of pulmonary fibrosis; these cells induce excessive proliferation and aberrant activation of fibroblasts, which ultimately generate an abundant extracellular matrix and collagen fibrin deposition. These characteristics are recognized by most researchers at present. The exact mechanism remains poorly understood, but many signaling pathways are involved.

Some research has revealed that the canonical Wnt signaling pathway, which is essential for fibroblast activation, is important in pulmonary fibrosis, and aberrant expression levels of endogenous Wnt antagonists are important regulating factors for activation of the Wnt signaling pathway [2–9]. As the commonest Wnt antagonists, secreted frizzled proteins (SFRPs) can competitively bind to the Wnt ligand or the Frizzled receptor and form nonfunctional complexes *via* a cysteine-rich domain (CRD), which is 30–50% identical to the Wnt ligand and the Frizzled binding domain [10]. The SFRPs are subdivided into two closely related subgroups according to gene sequence homology: SFRP1, SFRP2, and SFRP5 form one subgroup, whereas SFRP3 and SFRP4 form the other [11]. Downregulation of SFRPs is involved in various fibrotic diseases, such as skin fibrosis in systemic sclerosis [12], myocardial fibrosis [13], or renal fibrosis [14] in mice. On the other hand, upregulated SFRPs can inhibit proliferation of fibroblasts in different tissues [8,15,16], and reduce the production of extracellular cellulose [17] and apoptosis induced by cellular stress [18].

* Corresponding author at: Department of Rheumatology and Immunology, Beijing Chao-Yang Hospital, Capital Medical University, No. 8 Gong-Ti South Road, Chaoyang District, Beijing 100020, PR China.
E-mail addresses: zzyy90fs@126.com, zzyy90_fs@163.com (Z. Yi).

https://doi.org/10.1016/j.lfs.2018.12.041
Received 14 September 2018; Received in revised form 18 December 2018; Accepted 22 December 2018
Available online 23 December 2018

Growing evidence indicates a pivotal role of epigenetics in the onset and progression of pulmonary fibrosis [19–21]. As a classic epigenetic modification, DNA methylation, which predominantly occurs at the fifth carbon atom of cytosine residues of the CpG dinucleotide, is controlled by DNMTs, methyl-CpG-binding proteins, and other factors. The methylation-based modification may result in abnormal recombination of chromatin, and this process subsequently interferes with the recruitment of transcriptional coactivators and inhibits gene transcription as well [22]. Besides, DNA methylation changes are mostly mediated by DNA methyltransferases (DNMTs) in CpG islands, and this process mainly involves DNMT1, DNMT3A and DNMT3B in mammals. As an analog of 2′-deoxycytidine, the clinically used decitabine (5-aza-2′-deoxycytidine; hereafter: 5-aza) is reported to be the most effective inhibitor of DNA methylation [23,24] and can reactivate the expression of Wnt antagonists by reducing promoter hypermethylation [12,25].

The silenced or decreased expression of Wnt antagonists induced by promoter hypermethylation (which could activate Wnt signaling pathways) has been detected in some tumors and fibrotic diseases [12,25–27]. Although abnormal activation of the Wnt signaling pathway is also present in pulmonary fibrosis, changes of the expression and methylation of SFRPs in the course of this disease are still unknown. Therefore, the aim of our study was to assess the expression of Wnt antagonists (SFRPs) and their promoter methylation modification during pulmonary fibrosis.

2. Materials and methods

2.1. Establishment of experimental animal model

Male C57BL/6 mice of Specific Pathogen Free (SPF) grade, 7–8 weeks old, weighing about 20–25 g, were purchased from Beijing Vital Lihua Experimental Animal Technology Co., Ltd., and were used in all experiments. After conventional maintenance for a week, the mice underwent intratracheal instillation with 5.0 mg/kg bleomycin (Nippon Kayaku Co., Ltd., Tokyo, Japan) in 100 μl of normal saline (NS) for establishing a pulmonary fibrosis model as previously described [19,28]. The control animals were intratracheally injected with the same volume of NS. All procedures were approved by the Capital Medical University Animal Experiment and Experimental Animal Welfare Committee (ethical number: AEEI 2018007).

2.2. Animal grouping and model preparation

72 mice were randomly subdivided into an experimental group (BLM-group) and control group (NS-group). Ten to 12 mice were subjected to radiographic assessment of pulmonary fibrosis on Day 7 (D7), D14, and D21, then the mice were euthanized by excessive inhalation of isoflurane, and the serum and lung tissue were collected for subsequent experiments.

In the following experiment, the mice were randomly distributed into four groups (8 mice per group): NS + Vehicle group, NS + 5-aza group, BLM + Vehicle group, and BLM + 5-aza group. One day after bleomycin instillation, the mice were injected intraperitoneally with 5-aza (Selleck Chemicals, CAS number 2353-33-5) with 2.5 mg/kg every 2 days or 300 ul NS as a control [12]. On the 21st day, six to eight mice for each group were scanned by computed tomography (CT) and processed according to the above method.

2.3. Isolation and culture of primary lung fibroblasts

Primary lung fibroblasts from the mice were isolated and cultured as previously described [29,30]. Briefly, the lungs of mice at different times points were immersed in ice-cold 1 × PBS, and completely rid of the pleura and vessels immediately. After repeated rinsing, the lung tissue was cut into small tissue blocks of 1 × 1 mm size, which were placed in flasks and cultivated in the DMEM (Gibco) medium supplemented with 10% fetal bovine serum (FBS) (Gibco, USA), 1% of a penicillin-streptomycin solution (Lablead, China), and 1% L-glutamine (Caisson, USA). After lung fibroblasts migrated, the blocks were removed with forceps, and the primary lung fibroblasts were used in the subsequent experiment.

CT scanning of mouse lung.

All CT images were acquired and visualized in a Bruker SkyScan 1176 *in-vivo* micro-CT scanner (Bruker Corporation, Germany). The mice were scanned after inhalation anesthesia, and approximately 140 to 150 layers covered the entire lungs. Pulmonary density of images was assessed with Hounsfield units (HU) by methods published in other studies [31,32]. Briefly, 10 circles (regions of interest) with a diameter of 2 mm in the representative layers of the main bronchi (two circles), below the main bronchi (four circles), and below the trachea (four circles) were selected, with avoidance of the main vessels. Next, the average HU values of the circles in the three layers were calculated separately, which evaluated the pulmonary density of the upper, middle, and lower lung regions. The fibrosis in mouse lung CT images was calculated as described elsewhere [33,34]. And the scores on images were categorized into five grades according to the affected area: grade 0, no obvious tissue changes, no tissue patch or fibrosis; grade 1, mild changes, involved lung area is < 25%; grade 2, a moderate change, 25% to 50% of the lung is involved; grade 3, a severe change, 50% to 75% of the lung is involved; grade 4 terminal changes, the involved lung area is > 75%. These characteristic CT changes of ground-glass opacity, reticular pattern, and fibrosis stranding were evaluated separately. Then, the sum of the three indicator scores was calculated as the total pulmonary fibrosis score. Finally, the image analysis was independently evaluated by two investigators.

2.4. Histological examination

Fresh lung samples of mice were perfused and fixed with 4% paraformaldehyde (Solarbio, Beijing, China) for > 24 h. After dehydration, the samples were embedded in paraffin and sectioned at 4 μm thickness. The paraffin sections were stained with hematoxylin and eosin (HE) and Masson's reagent (Solarbio, Beijing, China). The degree of alveolitis was evaluated by HE staining according to the method of Szapiel et al. [35], with 0 meaning normal lung tissue; 1 denoted mild lung tissue inflammation, which meant that inflammatory cell infiltration was limited to local or near-pleural area, and the area was no > 20% of the lungs; 2 indicated moderate lung tissue inflammation: the affected area accounted for 20% to 50% of the whole lung; and 3 represented severe lung tissue inflammation, which meant that the affected area was > 50%. The severity of pulmonary fibrosis was scored by Masson staining, according to the standards of *Ashcroft* et al. [36]. The degrees of fibrosis were classified into grades 0–8, and the grade number corresponded to the score. Normal tissue was assigned a grade of 0, while the intensity of thickening of alveolar wall and bronchiolar vessels, with no damage to lung structure, was graded 2 or 3 depending on whether thickening was threefold relative to the norm. Formation of a fibrous mass and confluent distortion of structure was graded 4 or 5 depending on whether the affected area was > 10%. Severe contiguous fibrotic masses with the affected area being > 50% and formation of the air bubbles, which meant an alveolar cavity filled with fibrous tissue, were graded 6 or 7. Fibrous obliteration was graded 8. If there was any difficulty in scoring between two consecutive numbers, an intervening score was used.

2.5. Reverse transcription quantitative real-time polymerase chain reaction (RT-qPCR)

Total RNA was isolated from fresh lung samples of mice, and the primary lung fibroblasts were isolated using the Simple Total RNA Kit (Tiangen Biotech Co., Ltd., Beijing, China). The Revert Aid First Strand cDNA Synthesis Kit (Tiangen Biotech Co., Ltd., Beijing, China) was

Table 1
Sequences of primers used for PCR in this study.

Target	Primer sequence
SFRP1	Forward:5′-GAGCCGGTCATGCAGTTCTT-3′ Reverse:5′-GGCTTAGAGGCTTCCGTGGT-3′
SFRP2	Forward:5′-AACGACATCAACGCTCCGTA-3′ Reverse:5′-TGCGCTTGAACTCTCTCTGG-3′
SFRP3	Forward:5′-GCTGCCTCTGTCCTCCACTT-3′ Reverse:5′-CAAGCCGATCCTTCCACTTC-3′
SFRP4	Forward:5′-CTCCATCCTGGTGGCGTTAT-3′ Reverse:5′-CGTTCTCCTGAGTGCTGTGG-3′
SFRP5	Forward:5′-ATGCTGCACTGCCACAAGTT-3′ Reverse:5′-TGTGCTCCATCTCACACTGG-3′
β-catenin	Forward:5′-GGCAACCCTGAGGAAGAAGA-3′ Reverse:5′-AGCGTCAAACTGCGTGGAT-3′
DNMT1	Forward:5′-ATTCCACCAAGCAGGCATCT-3′ Reverse:5′-AAGCACGTTGCAGTCCTCTG-3′
COL1	Forward:5′-TCGTGGTGAGACTGGTCCTG-3′ Reverse:5′-TGTCACCTTGTTCGCCTGTC-3′
α-SMA	Forward:5′-GAGCATCCGACACTGCTGAC-3′ Reverse:5′-GCACAGCCTGAATAGCCACA-3′
β-actin	Forward:5′-TGGAATCCTGTGGCATCCATGAAAC-3′ Reverse:5′-TAAAACGCAGCTCAGTAACAGTCCG-3′

SFRP1: secreted frizzled-related protein1, *SFRP2*: secreted frizzled-related protein 2, *SFRP3*: secreted frizzled-related protein3, *SFRP4*: secreted frizzled-related protein 4, *SFRP5*: secreted frizzled-related protein5, *DNMT1*: DNA methyltransferase 1, *COL1*: collagen I, *α-SMA*: α-smooth muscle actin.

employed for RNA reverse transcription, and the SYBR Prime Script RT-PCR Kit (Takara Biotechnology Co., Ltd., Dalian, China) for quantitative PCR (qPCR). RT-qPCR was implemented on an ABI Prism 7500 instrument (Applied Biosystems, Foster City, CA, USA) with the predesigned primers (the sequences of the primers are listed in Table 1). The gene transcription was quantified *via* a standard curve by the comparative Ct method with normalization to β-actin transcription. The $2^{-\Delta Ct}$ method (ΔCt = Ct of gene − Ct of *β-actin*) was used [37]. All samples were examined in triplicate, and the experiment was repeated at least three times.

2.6. Western blot

Total protein of collected lung tissues and cells was extracted with the Nuclear and Cytoplasmic Protein Extraction Kit (Beyotime Biotech Co., Ltd., Shanghai, China). Samples, after quantification quantified by the BCA method, were loaded onto gels, electrophoretically separated by sodium dodecyl sulfate polyacrylamide gel electrophoresis (SDS-PAGE), and transferred onto a polyvinylidene fluoride (PVDF) membrane (Roche Diagnostics Corporation, Indianapolis, IN, USA) using an electrophoresis system (Bio-Rad, Hercules, CA, USA). The membranes were sheared, and after blockage with 5% nonfat milk for 1 h at room temperature, they were separately incubated with primary antibodies overnight at 4 °C. Antibodies against the following proteins were employed: SFRP1 (1:200, cat. Ab4193, Abcam, Cambridge, UK), SFRP4 (1:1000, cat. Ab154167, Abcam, Cambridge, UK), DNMT1 (1:1000, cat. Ab188453, Abcam, Cambridge, UK), COL1 (1:500, cat. Ab21286, Abcam, Cambridge, UK), α-SMA (1:1000, cat. Ab5694, Abcam, Cambridge, UK), β-actin (1:3000, cat. 3700S, Cell Signaling Technology; Boston, USA). Then, a secondary antibody, *i.e.*, a horseradish peroxidase–conjugated goat anti-rabbit IgG antibody (1:2000, cat. A0208. Beyotime Biotech, Shanghai, China), was applied. The bands were visualized on a double infrared laser scanning imaging system (LI-COR Biosciences, Lincoln, NE, USA). The semi-quantitative results out of these Western blot films were calculated by image J software (version 1.42, National Institutes of Health, USA), and the relative expression levels of these proteins were respectively normalized to their internal control of β-actin. The measurement of intermembrane (IM) normalization was used to balance the difference among gels [38,39].

Table 2
Sequences of primers for methylation (M) and unmethylation (U) DNA.

Target		Primer sequence
SFRP1	Methylation	Forward:5′-TTAGGGTTCGGTTATTCGTATATC-3′ Reverse:5′-ACCGAATACTATCCCGACTCG-3′
	Unmethylation	Forward: 5′-GATTTAGGGTTTGGTTATTTGTATATTG-3′ Reverse:5′-AAACCAAATACTATCCCAACTCAC-3′
SFRP4	Methylation	Forward:5′-GTTGTTGAGTTTACGTTAGGGGAC-3′ Reverse:5′-GCGAAAAACTCCAATCTCGAA-3′
	Unmethylation	Forward:5′-GGTTGTTGAGTTTATGTTAGGGGAT-3′ Reverse:5′-CCACAAAAAACTCCAATCTCAAA-3′

SFRP1: secreted frizzled-related protein 1, SFRP4: secreted frizzled-related protein 4.

2.7. Methylation-specific PCR

Genomic DNA was isolated from fresh lung samples of mice by means of the TIANamp Genomic DAN Kit (Tiangen Biotech Co., Ltd., DP304, Beijing, China) (10 to 12 mice from each group). For bisulfite transformation of DNA, 200 ng of genomic DNA was processed using the Sodium Bisulfite Kit (Tiangen Biotech Co., Ltd., DP5, Beijing, China). The sequences of the primer pairs for SFRP1 and SFRP4, which were used for amplification of methylated (M)- and unmethylated (U) DNA, were designed in the Methprimer Software (Li and Dahiya, 2002) and are listed in Table 2. PCR was conducted with the Methylation Specific PCR Kit (Tiangen Biotech Co., Ltd., EM101, Beijing, China) with an initial denaturation step of 95 °C for 5 min, followed by 35 cycles of denaturation at 94 °C for 20 s, annealing at the respective T_m for each set of primers (60 °C for SFRP1 and 62 °C for SFRP4) for 30 s, and extension at 72 °C for 5 min. Next, the mixed amplified products (5 μl for each reaction) and ethidium bromide (1 μl for each reaction) were loaded onto a 2% agarose gel, subjected to electrophoresis, and visualized under ultraviolet illumination. The methylation status of SFRP1 and SFRP4 was investigated as previously described [40] and the methylation rate (M / (M + U)) was calculated according to the promoter methylation status within each group of mice.

2.8. Statistical analysis

The statistical software package (SPSS 19.0; SPSS, Inc., Chicago, IL, USA) was used, and the results were expressed as mean ± SD. The *t*-test for comparison of two groups and One-way analysis of variance (ANOVA) and Scheffe *Post Hoc* Tests for multiple group comparisons were used. The correlation between the data was analyzed, and the linear correlation coefficient was calculated by Spearman's formula. Values at $p < 0.05$ were considered statistically significant.

3. Results

3.1. The SFRP1 and SFRP4 were downregulated in bleomycin-induced pulmonary fibrosis in mice

The comprehensive assessment of histopathology (Fig. S1), biochemical methods (Fig. S2), and lung CT imaging (Fig. S3) were conducted to verify the significant increased alveolitis and pulmonary fibrosis in C57BL/6 mice treated with bleomycin, when compared with the control group (saline injection), at D7, D14, and D21 (see online Supplementary Data 1).

Over the course of pulmonary fibrosis in mice, we found that the transcription of *SFRP1* and *SFRP4* significantly changed. When compared with the control group, the transcription of *SFRP1* decreased significantly at D14 (2.65 ± 0.53 *vs.* 1.34 ± 0.63, $p < 0.01$) and D21 (2.75 ± 0.66 *vs.* 1.06 ± 0.57, $p < 0.001$), and the level gradually decreased during the course of pulmonary fibrosis (D7 *vs.* D14 *vs.* D21:

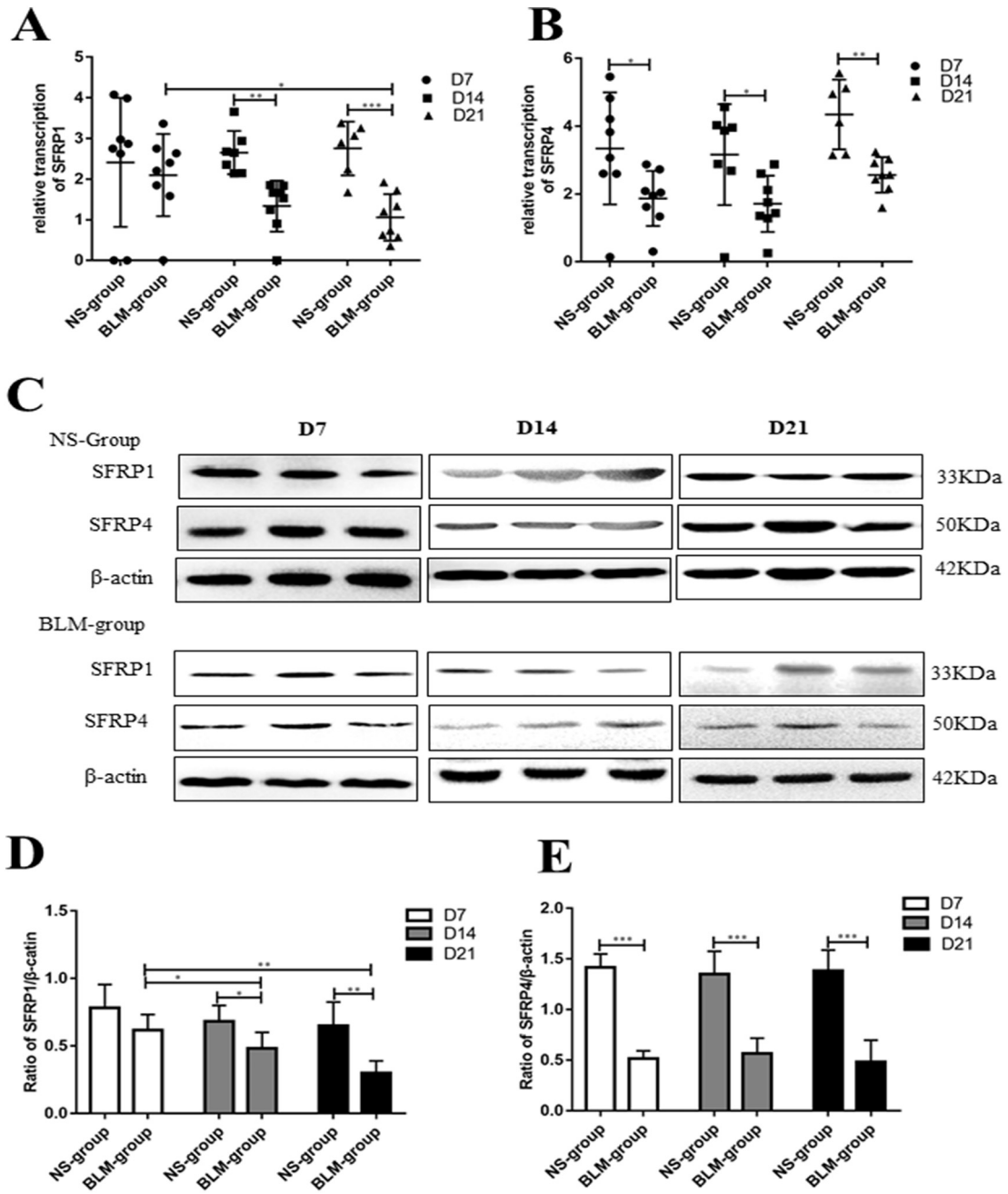

Fig. 1. The expression levels of SFRP1 and SFRP4 were downregulated in lung tissue of bleomycin-induced pulmonary fibrosis in mice. The relative expression levels of SFRP1 and SFRP4 of lung tissue from the NS-group and BLM-group were evaluated by Western blotting (C) and RT-qPCR (A and B) at D 7, D 14 and D 21 respectively. D and E: the ratios of expression levels of SFRP1 and SFRP4 to β-actin, which were subsequently normalized by the IM normalization of the average signal value of β-actin at D7. Six to eight mice were randomly selected from each group. Graphs showed mean ± SD for each group. $^{*}p < 0.05$, $^{**}p < 0.01$, $^{***}p < 0.001$.

2.10 ± 1.01 *vs.* *1.34 ± 0.63* *vs.* 1.06 ± 0.57, $p < 0.05$). Accordingly, the protein expression of SFRP1 gradually decreased as well (*D7 vs. D14 vs. D21*: 0.60 ± 0.14 *vs.* 0.48 ± 0.12 *vs.* 0.27 ± 0.08, $p < 0.01$). Meanwhile, the transcription (3.34 ± 1.65 *vs.* 1.87 ± 0.81, $p < 0.01$) and protein expression (1.42 ± 0.13 *vs.* 0.52 ± 0.08, $p < 0.001$) of SFRP4 decreased significantly at D7, and stayed lowered over the course of the disease (D7 *vs.* D14 *vs.* D21, mRNA expression: 2.09 ± 0.60 *vs.* 1.89 ± 0.69 *vs.* 2.56 ± 0.62, $p = 0.069$, protein expression: 0.52 ± 0.08 *vs.* 0.57 ± 0.15 *vs.* 0.48 ± 0.21, $p = 0.66$), as shown in Fig. 1. The low transcription levels of *SFRP2*, *−3* and *−5* did not represent a significant difference between the experimental group and control group (Fig. S4).

To evaluate the relation between pulmonary fibrosis and abnormal expression of SFRP1 and SFRP4, we conducted the correlation analysis (see online Supplementary Data 3). The changes in expression of SFRP1 and SFRP4 were associated with fibrotic lesions (Fig. S4), which negatively correlated with fibrosis scores based on pathology (SFRP1: $r = -0.526$, $p < 0.01$, SFRP4: $r = -0.711$, $p < 0.001$), and fibrosis scores based on CT images (SFRP1: $r = -0.566$, $p < 0.01$, SFRP4: $r = -0.433$, $p < 0.05$). In addition, the altered expression of SFRP1 and SFRP4 was negatively associated with alveolitis scores (SFRP1: $r = -0.377$, $p < 0.05$, SFRP4: $r = -0.427$, $p < 0.01$).

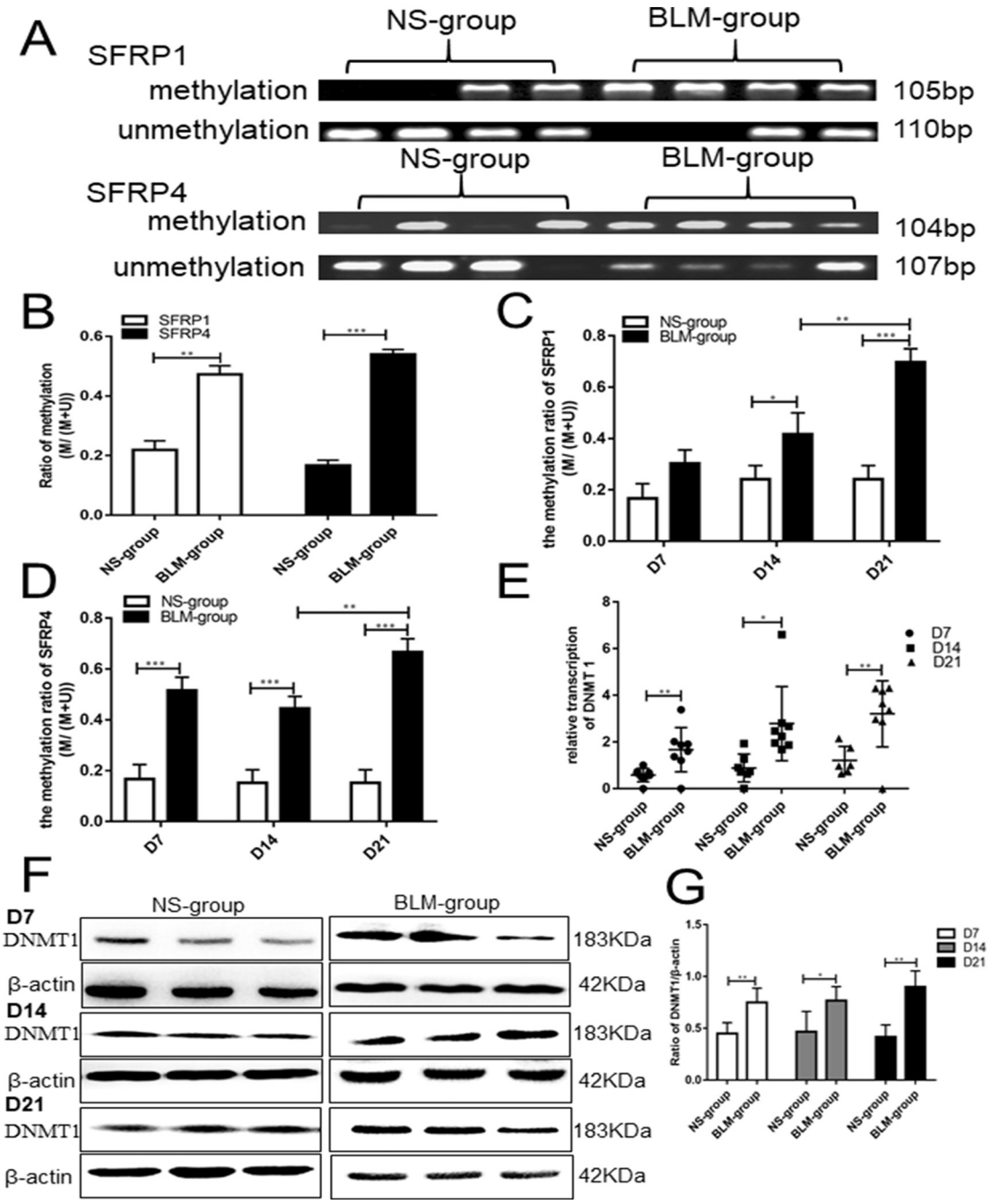

Fig. 2. The promoters of *SFRP1* and *SFRP4* were hypermethylated in lungs from BLM-treated mice (BLM-group) when compared with the NS-group (the control). (A) Representative images of agarose gels of the methylation-specific PCR products (M) and unmethylated PCR products (U) from eight samples were shown. (B) The relative ratios of methylation (M / (M + U)) of *SFRP1* and *SFRP4* were higher in the BLM-group than in the control. (C) and (D) The changes of relative ratios of methylation of *SFRP1* or *SFRP4* in the course of pulmonary fibrosis in mice (10 to 12 mice were randomly selected from each group). (E) and (F) The relative expression levels of DNMT1 in the lung tissue from the NS-group and BLM-group were evaluated by RT-qPCR (E) and Western blotting (F) at D7, D14, and D21 respectively. (G) The ratios of expression levels of DNMT1 to β-actin were shown, which were subsequently normalized by the IM normalization of the average signal value of β-actin at D7 (six to eight mice were randomly selected from each group). Data were obtained from three independent experiments. * $p < 0.05$, ** $p < 0.01$, *** $p < 0.001$.

3.2. Promoters of SFRP1 and SFRP4 were hypermethylated in the lungs of bleomycin-treated mice

Epigenetics is an important regulatory mechanism for the expression of SFRPs. Besides, according to various reports [12,49,51], MSP is a sensitive method for detection of promoter methylation of *SFRP* genes. Hence, the methylation states of promoters, including those of *SFRP1* and *SFRP4*, were analyzed by MSP in this study. The methylation rates of *SFRP1* promoter (0.22 ± 0.03 *vs.* 0.47 ± 0.03, $p < 0.01$) and *SFRP4* promoter (0.17 ± 0.02 *vs.* 0.54 ± 0.02, $p < 0.001$) were significantly higher than those in the control group (Fig. 2A, B). The promoter methylation of *SFRP1* occurred at D14 (0.24 ± 0.05 *vs.* 0.42 ± 0.08, $p < 0.05$, relative to the control), and the rate gradually increased over the course of the disease (*D7 vs. D14 vs. D21:* 0.30 ± 0.05 *vs.* 0.42 ± 0.08 *vs.* 0.70 ± 0.05, $p < 0.001$). In contrast, the hypermethylation of *SFRP4* occurred at D7 already (0.17 ± 0.06 *vs.* 0.52 ± 0.05, $p < 0.001$, relative to control), and there was a sustained decrease over the course of the disease (*D7 vs.*

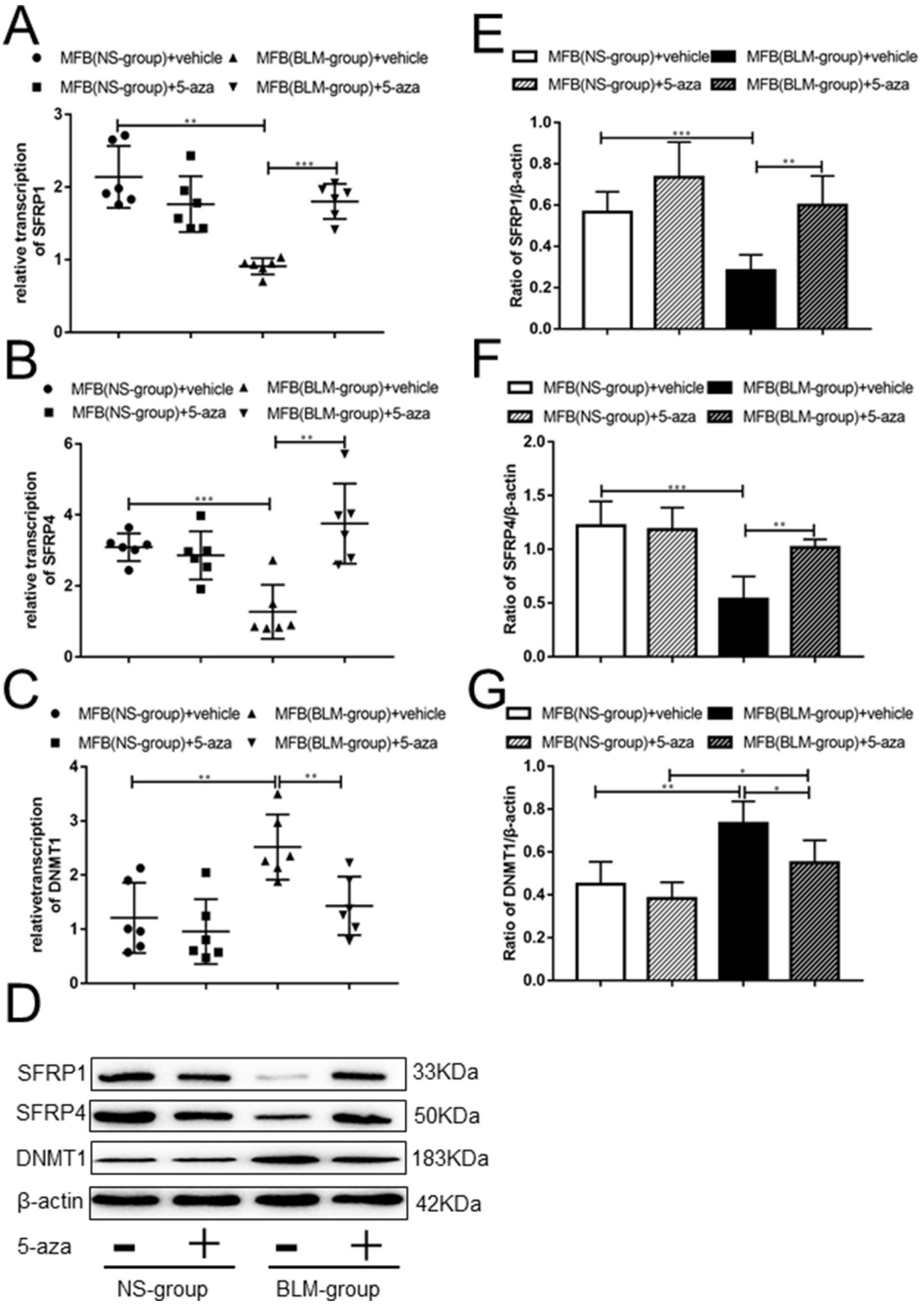

Fig. 3. Downregulation of SFRP1 and SFRP4 were prevented by inhibition of DNA methyltransferases. The primary lung fibroblasts (FB) of the NS-group (at D 21) and BLM-group (at D 21) were incubated with 5-aza at a dose of 5 μM for 24 h. The expression of SFRP1, SFRP4 and DNMT1 was evaluated by RT-qPCR (A, B, and C) and Western blotting (D). The relative expression levels of SFRP1 (E), SFRP4 (F) and DNMT1 (G) were normalized to the internal control of β-actin, and the IM normalization was used to balance the difference among gels. Graphs show mean ± SD for each group (n = 6 each). Data were obtained from three independent experiments. $^{*}p < 0.05$, $^{**}p < 0.01$, $^{***}p < 0.001$.

D14 vs. D21: 0.52 ± 0.052 *vs.* 0.44 ± 0.048 *vs.* 0.66 ± 0.053, $p < 0.01$) (Fig. 2C, D). Furthermore, we also found the transcription (*D21*: 1.21 ± 0.60 *vs.* 3.66 ± 0.67, $p < 0.001$) and protein expression (*D21*: 0.42 ± 0.12 *vs.* 0.90 ± 0.15, $p < 0.01$) of DNMT1, which might facilitate DNA hypermethylation, also significantly increased in the fibrosis model during the study period (Fig. 2E–G).

To confirm that the decreases of transcription and protein expression of SFRP1 and SFRP4 are due to hypermethylation, we incubated a DNA methyltransferase inhibitor (5-aza) with the primary lung fibroblasts that were isolated from the bleomycin group and the control

group. As presented in Figs. 3, 5-aza significantly inhibited the transcription (*bleomycin group vs. bleomycin + 5-aza group*: 2.52 ± 0.60 *vs.* 1.43 ± 0.54, $p < 0.05$) and protein expression (*bleomycin group vs. bleomycin + 5-aza group:* 0.73 ± 0.10 *vs.* 0.55 ± 0.11, $p < 0.05$) of DNMT1. When compared with the NS group, the transcription (*SFRP1:* 2.14 ± 0.43 *vs.* 0.91 ± 0.11, $p < 0.01$ and *SFRP4:* 3.09 ± 0.39 *vs.* 1.27 ± 0.76, $p < 0.001$) and protein expression (*SFRP1:*0.62 ± 0.10 *vs.* 0.28 ± 0.08, $p < 0.01$, *SFRP4:* 1.25 ± 0.23 *vs.* 0.58 ± 0.21, $p < 0.001$) of SFRP1 and SFRP4 significantly decreased. Nonetheless, after incubation with 5-aza, the impairment of transcription (*SFRP1:* 0.91 ± 0.11 *vs.* 1.80 ± 0.24, $p < 0.001$, *SFRP4:* 1.27 ± 0.76 *vs.* 3.76 ± 1.13, $p < 0.01$) and of protein expression (*SFRP1:* 0.28 ± 0.08 *vs.* 0.60 ± 0.14, $p < 0.01$, *SFRP4:* 0.58 ± 0.21 *vs.* 1.02 ± 0.08, $p < 0.01$) of SFRP1 and SFRP4 in fibroblasts from the bleomycin was attenuated, and these parameters became almost comparable to those of fibroblasts from the control group.

Thus, in the model of pulmonary fibrosis, the downregulated mRNA and protein levels of SFRP1 and SFRP4 are related to the hypermethylation of their promoters at different stages of the disease. And the inhibitor of DNMTs (5-aza) could reactivate the expression of SFRP1 and SFRP4.

3.3. 5-Aza can downregulate β-catenin in vivo and in vitro

As the key regulatory protein, β-catenin is always used as the marker for activation of canonical Wnt signaling pathway. In this study, the upregulated transcription (2.14 ± 0.49 *vs.* 3.46 ± 0.66, $p < 0.01$) and protein expression (0.97 ± 0.14 *vs.* 1.30 ± 0.21, $p < 0.01$) of β-catenin were verified in the primary lung fibroblasts from the bleomycin-treated group. After incubated with 5-aza, the transcription of *β-catenin* significantly decreased (3.46 ± 0.66 *vs.* 2.44 ± 0.41, $p < 0.01$). In the subsequent analysis of experimental lung tissue, treatment with 5-aza prevented the bleomycin-induced increase in the transcription (3.94 ± 0.71 *vs.* 2.86 ± 0.59, $p < 0.05$) and protein expression (1.62 ± 0.16 *vs.* 0.92 ± 0.16, $p < 0.01$) of β-catenin. In contrast, 5-aza had only a minor effect on β-catenin in the control mice, as shown in the Fig. 4.

DNMT inhibitors can reduce the pulmonary fibrosis in the bleomycin-treated mice.

As depicted in Fig. 5, the intraperitoneal injection of 5-aza significantly reduced alveolitis scores (2.09 ± 0.60 *vs.* 1.36 ± 0.35, $p < 0.05$) and fibrosis scores (4.13 ± 1.87 *vs.* 2.46 ± 0.78, $p < 0.05$) (Fig. 5A–D) in the lungs of mice challenged with bleomycin. Besides, this treatment downregulated the transcription of *CLO1a1* (6.76 ± 2.17 *vs.* 4.07 ± 0.98, $p < 0.05$) and *α-SMA* (9.18 ± 2.02 *vs.* 6.52 ± 2.10, $p < 0.05$), as well as the protein expression of CLO1a1 (1.65 ± 0.27 *vs.* 1.00 ± 0.23, $p < 0.01$) and α-SMA (1.87 ± 0.36 *vs.* 1.22 ± 0.21, $p < 0.01$) (Fig. 5E–I). Besides, the pulmonary densities on lung CT images of the upper part of the lung (−378 ± 70 *vs.* −560 ± 20, $p < 0.001$), of the middle part of the lung (−430 ± 46 *vs.* −667 ± 51, $p < 0.001$), and of the lower part of the lung (−385 ± 34 *vs.* −670 ± 47, $p < 0.001$) decreased in the mice with pulmonary fibrosis challenged with 5-aza, as did the pulmonary fibrosis scores (9.21 ± 2.09 *vs.* 5.76 ± 2.29, $p < 0.01$) according to the images (Fig. 6). Furthermore, as for the side effects, the treatment with 5-aza had a minor effect on weight in the control group (2.80 ± 0.71 *vs.* 0.33 ± 3.10, $p > 0.05$), but significantly attenuated the body weight loss in the bleomycin group (−2.89 ± 4.67 *vs.* 2.39 ± 1.43, $p < 0.05$) (Fig. 6F).

4. Discussion

In this study, we demonstrated the changes in protein expression, in transcription, and promoter methylation of *SFRP1* and *SFRP4* in lung tissues of mice with pulmonary fibrosis induced by bleomycin, hoping to determine the significance of promoter methylation in the regulation of Wnt antagonists in pulmonary fibrosis. First, a comprehensive assessment of histopathology, biochemical assays, and lung CT imaging confirmed the increased fibrosis and inflammation in the mouse model of bleomycin-induced pulmonary fibrosis. Second, the significantly increased promoter methylation of *SFRP1* and *SFRP4* resulted in their impaired transcription and decreased protein expression during pulmonary fibrosis in the mice, whereas 5-aza induced demethylation and reactivated *SFRP1* and *SFRP4 in vitro*. Third, the DNMT inhibitor effectively attenuated activation of β-catenin and reduced pulmonary fibrosis in this mouse model.

As a classic animal model, the mice with pulmonary fibrosis induced by a single dose (tracheal administration) of bleomycin are widely used in research. In this study, we performed comprehensive assessment of histopathology, biochemical methods, and lung CT imaging to evaluate the fibrosis and inflammation in murine lungs and to confirm the successful establishment of the pulmonary-fibrosis model. After that, the changes in alveolitis and pulmonary fibrosis were found to be similar to our previously published findings [19,28,31]. Besides, this study revealed that the mice with pulmonary fibrosis induced by bleomycin have an overactive Wnt signaling pathway [41], which provides the foundation for studies on the effects of regulatory factors related to Wnt signaling *in vitro*.

Resent research proved that aberrant activation of the Wnt signaling pathway is associated with decreased amounts of Wnt antagonists in many fibrotic diseases. In our study, the detected SFRPs belong to one important group of endogenous antagonists of the Wnt signaling pathway. Our results revealed that in the model of pulmonary fibrosis, the transcription and protein expression of SFRP1 and SFRP4 both decreased; the downregulation of SFRP1 mainly occurred at D14 and D21, and reduced SFRP4 expression was observed already at D7. Moreover, the expression levels of SFRP1 and SFRP4 separately correlated with fibrosis scores based on histopathology and fibrosis scores based on lung CT images (Fig. S5A-D). After the subsequent treatment with 5-aza *in vitro*, we observed that the decreased expression of β-catenin (which is the central integrator of canonical Wnt signaling) was accompanied by the reactivated expression of SFRP1 and SFRP4. Besides, the antifibrotic effects of SFRP1 and SFRP2 have been confirmed in some models of fibrotic diseases, and a lack of SFRP1 expression induces cardiomyocyte fibrosis in heart [13] and causes proliferation of lung mesenchymal cells [42], whereas a loss of SFRP4 promotes the thickening of skin in mice [43]. In contrast, increased expression of SFRP1 can inhibit the proliferation of lung fibroblasts *via* culture supernatants of mesenchymal stem cells [8], and increased SFRP4 expression depresses the proliferation of fibroblasts derived from the systemic sclerosis patient's skin [44]. Therefore, SFRP1 and SFRP4 may play an important role in the onset and progression of pulmonary fibrosis.

Furthermore, we noticed that the expression levels of SFRP1 and SFRP4 separately correlated with alveolitis scores (Fig. S5E and F); this finding is consistent with the reports that an increased SFRP1 protein level can relieve inflammation in ischemic heart disease by reducing neutrophil infiltration [45], Whereas reduced SFRP4 expression causes inflammation in adipose tissue by inhibiting the formation of capillaries [46]. Hence, SFRPs may not only affect fibrosis but also participate in the regulation of inflammatory. Therefore, the potential significance of SFRPs in pathogenesis of pulmonary fibrosis needs further study in consideration of the coexisting inflammation and fibrosis.

Converging lines of evidence suggest that DNA methylation is widely present and performs an important function in the pathogenesis of pulmonary fibrosis, according to epigenetics analysis at the levels of lung tissue and fibroblasts [47,48]. Further analysis on the functional changes in fibroblasts under the influence of aberrant methylation has revealed that epigenetic modification of *THY-1* promotes the conversion of lung fibroblasts to myofibroblasts [49], whereas hypermethylation of *E*-prostaglandin 2 decreases the expression of a specific receptor on the fibroblast surface, thereby leading to prostaglandin E2

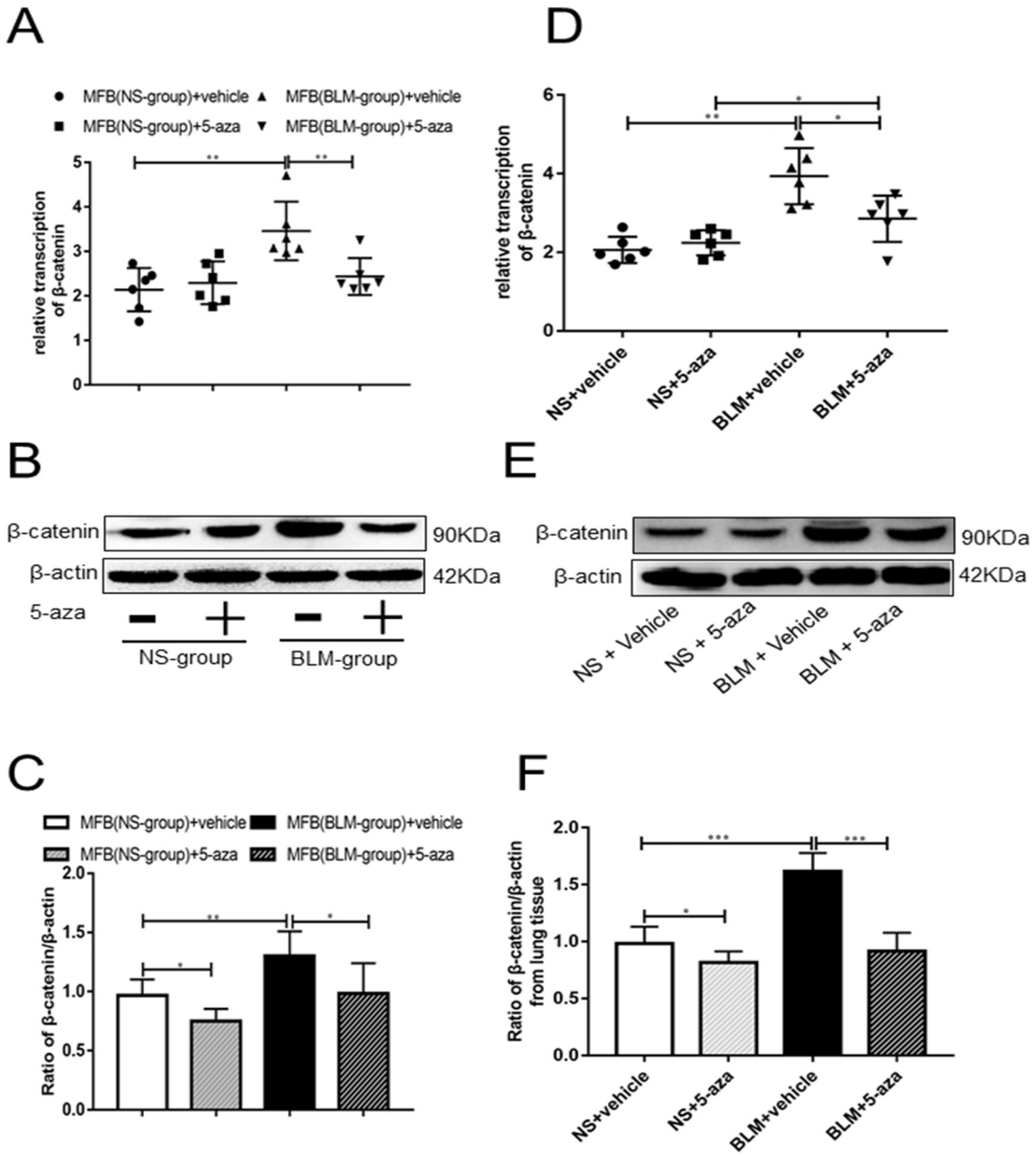

Fig. 4. Inhibition of DNA methyltransferases reduced β-catenin *in vitro* and *in vivo*. The relative expression levels of β-catenin from primary fibroblasts (FB), incubated with 5-aza, were evaluated by RT-qPCR (A) and Western blotting (B, C) (n = 6 each). The relative expression levels of β-catenin from lung tissue in mice were evaluated by RT-qPCR (D) and Western blotting (E and F) (n = 6 each), and the IM normalization was used to balance the difference among gels. Graphs show mean ± SD. $^{*}p < 0.05$, $^{**}p < 0.01$, $^{***}p < 0.001$.

resistance [50]. In addition, hypermethylation of proapoptotic gene *p14 (ARF)* is associated with the increased antiapoptotic ability of lung fibroblasts [51]. In our study, the promoters of *SFRP1* and *SFRP4* were mostly hypermethylated in the lung tissues from bleomycin-treated mice. Although the significant promoter hypermethylation of *SFRP1* mainly occurred at D14 and D21, and the aberrant methylation of *SFRP4* already took place at D7; these events paralleled the down-regulated protein expression of SFRP1 and SFRP4 at different time points. Next, interventions *in vitro* revealed that the aberrant promoter methylation could be reversed by DNMT inhibitors, as confirmed by subsequently reactivated expression of SFRP1 and SFRP4. Besides, several studies suggest that that the promoter hypermethylation of SFRP1 is an important factor of skin fibrosis in patients suffered systemic sclerosis [12], and aberrant methylation of *SFRP1* and *SFRP2* is a key cause of hyperproliferative fibroblasts in lesions of patients with skin scars [25]. Therefore, an epigenetic modification, for instance, DNA methylation, may induce severe downregulation of Wnt antagonists, thus possibly facilitating the onset and progression of fibrosis.

In our study, *SFRP1* and *SFRP4* in mice with bleomycin-induced pulmonary fibrosis also manifested promoter hypermethylation and decreased expression, whereas a challenge with 5-aza 1 day after bleomycin instillation restored their expression *in vitro* and alleviated experimental pulmonary fibrosis in mice. The generally accepted mechanism is as follows: 5-aza can be metabolized to form a triphosphate deoxynucleotide *in vivo*, which may bind to DNMT and take place of cytosine because of the strong affinity [23,52]. Through the competitive binding to DNMT, 5-aza might block hypermethylation by reducing the methylation at a CpG site and reviving transcription of a target gene, and finally reverse the methylation effects in fibrosis.

Now, 5-aza, as the strongest methyltransferase inhibitor (which is clinically used to regulate methylation in myelodysplastic syndromes (MDS) [53]), was proved to alleviate fibrosis in several animal models.

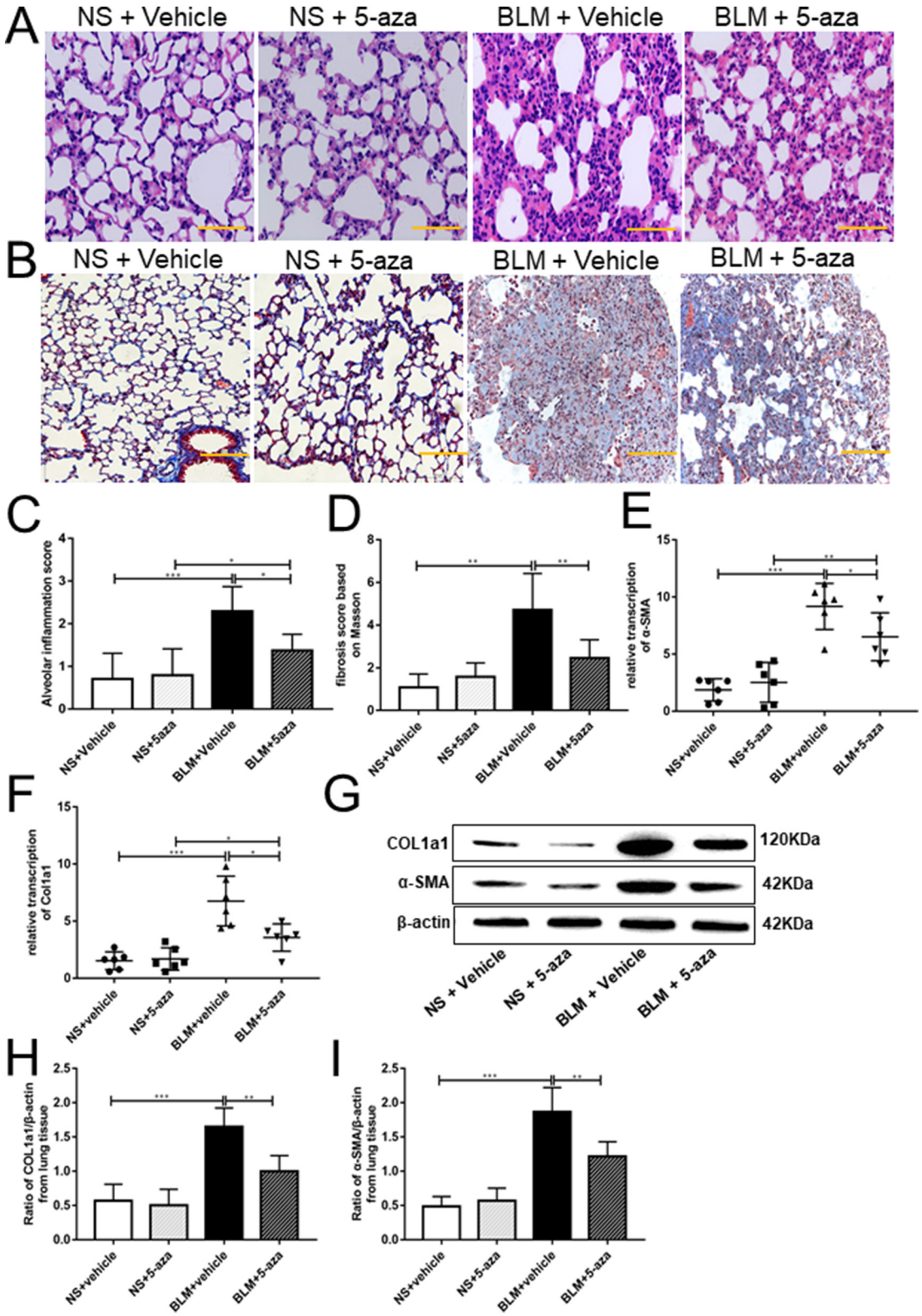

Fig. 5. Inhibition of DNA methyltransferases alleviated bleomycin-induced pulmonary fibrosis in mice. Representative HE-stained (A) at ×400 magnification and Masson-stained (B) tissue sections at ×200 magnification at D21 were shown. The semi-quantitative alveolitis score (C) and fibrosis score (D) were determined by two investigators in a blinded manner. The scale bar is 5 μm in (A) and 10 μm in (B). The relative transcriptional and expression levels of COL1a1 and α-SMA of lung tissue were evaluated by RT-qPCR (E and F) and Western blotting (G–I) at D21 (n = 6 each), and the IM normalization was used to balance the difference among gels. Graphs showed mean ± SD for each group. Data were obtained from three independent experiments. $^{*}p < 0.05$, $^{**}p < 0.01$, $^{***}p < 0.001$.

Appropriate administration of 5-aza can attenuate angiotensin II–induced cardiac fibrosis in mice [54] and reduce fibrosis in the left ventricle; the latter change improves ECG arrhythmic profiles and superoxide dismutase activities in spontaneously hypertensive rats [55] and restores the MMP-9/TIMP-1, TIMP-2 balance during hyperhomocysteinemia, thereby inhibiting extracellular-matrix remodeling and

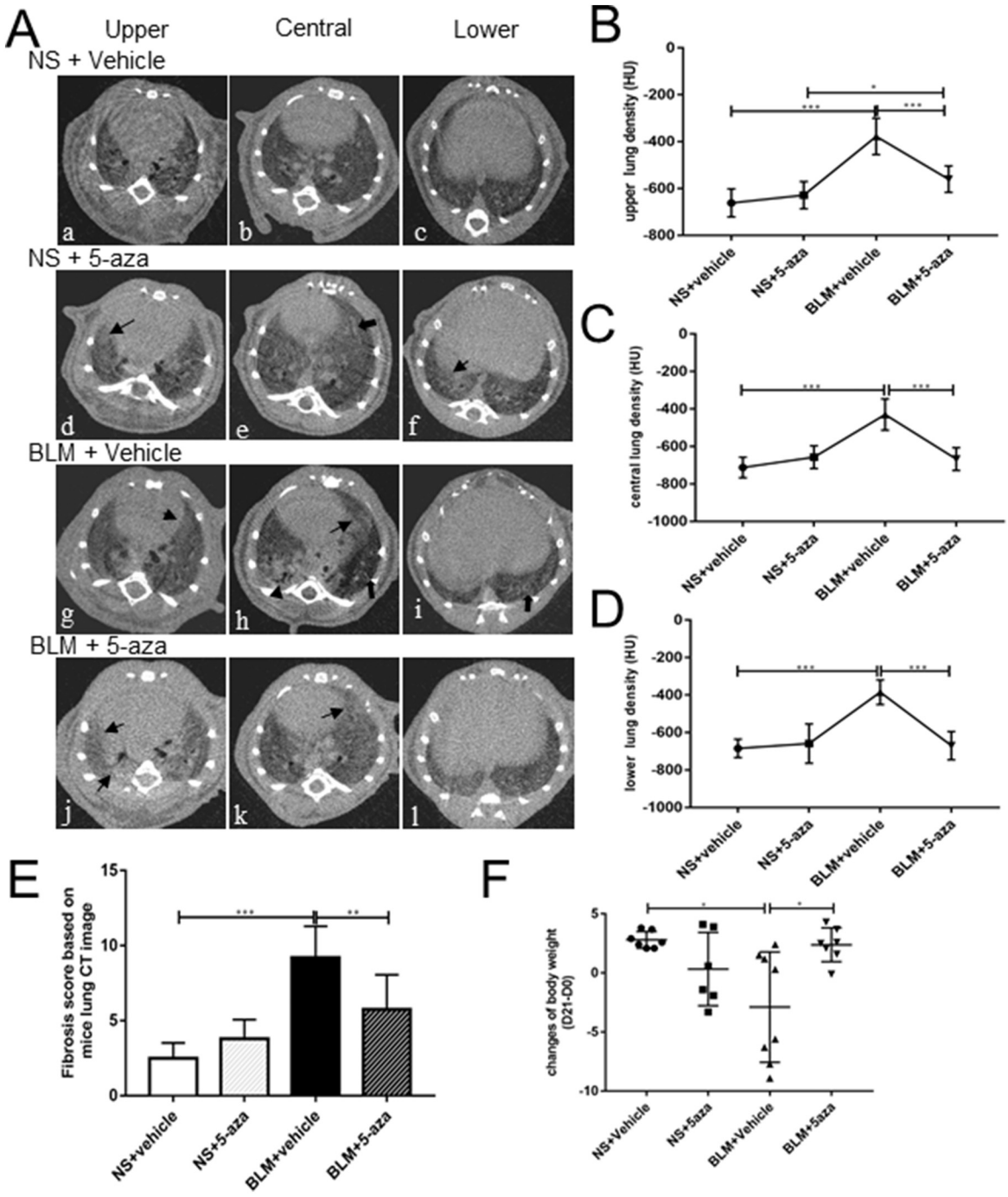

Fig. 6. Inhibition of DNA methyltransferases alleviated lung damage and fibrosis in mice according to CT images. Lung density of the upper, central and lower region of the lung was measured and expressed in HU according to a previously descripted method [31,32]. (A) Representative CT images of the four groups of animals (n = 6 each) at Day 21. Quantification of lung density was performed on the upper (B), middle (C), and lower (D) pulmonary regions. (E) The fibrosis score of a CT image of a murine lung was also assessed, which took into account the following characteristic CT changes: ground-glass opacity (thin arrow), a reticular pattern (bold arrow) and fibrosis stranding (triangle). Image analysis was performed by two investigators independently and blindly. (F) Changes of body weight were evaluated (n = 7 for the NS + Vehicle group, n = 6 for the NS + 5-aza group, n = 8 for the BLM + Vehicle group, and n = 7 for the BLM + 5aza group). Graphs show mean ± SD for each group. $^{*}p < 0.05$, $^{**}p < 0.01$, $^{***}p < 0.001$.

renal fibrosis [56]. Nonetheless, as for the fibrosis in chronic kidney disease induced by ischemia, subcutaneously administered 5-aza fails to attenuate fibrosis; this phenomenon might be related to the short-term employment of 5-aza [57]. Because DNA methylation is a potentially reversible process, systemic administration of 5-aza may relieve transcriptional repression of key genes and improve disease outcomes; these data may provide a new potential direction for the treatment of pulmonary fibrosis. Moreover, as a clinically used antitumor drug, 5-aza has fairly good tolerability, and in our study, intraperitoneal administration of 5-aza did not cause a significant weight loss.

Our study has several important limitations. First, a variety of Wnt protein subtypes and receptor subtypes undergo changes in pulmonary fibrosis; with which subtypes SFRPs (SFRP1 and SFRP4) interact and on which subtypes they exert biological function is still unclear, and these need further research. Second, as for the complexity of the pathogenesis of pulmonary fibrosis, intraperitoneal injection of a DNMT inhibitor (5-

aza) can not only modify the methylation of *SFRP1* and *SFRP4*, but also regulate methylation of other genes in general, and the mechanism *via* which DNMT inhibitors alleviate pulmonary fibrosis is worth further research.

5. Conclusion

In summary, promoter hypermethylation may downregulate *SFRP1* and *SFRP4* at different stages of pulmonary fibrosis and may overactivate the Wnt signaling pathway and participate in the onset and progression of pulmonary fibrosis. Furthermore, DNMT inhibitors can effectively attenuate the activated β-catenin expression and reduce fibrosis in mice. Together with our previous research into the effects of histone acetylation and deacetylases on pulmonary fibrosis [19], the present study suggests that the importance of epigenetic modifications cannot be ignored and may provide a possible new direction for the research on treatments of pulmonary fibrosis.

Author' contributions

JFZ and QF were involved in the design and implementation of this experiment, and YZ supervised and was responsible for the analysis of the data. The three authors jointly drafted and revised the manuscript, and provided final approval of the version to be published. All the authors read and approved the final manuscript.

Acknowledgments

This work received financial support from the National Natural Science Foundation of China (No. 81471616).

Competing interests

All authors declared no conflicts of interests.

Appendix A. Supplementary data

Supplementary data to this article can be found online at https://doi.org/10.1016/j.lfs.2018.12.041.

References

[1] A. Fischer, K.M. Antoniou, K.K. Brown, et al., An official European Respiratory Society/American Thoracic Society research statement: interstitial pneumonia with autoimmune features, Eur. Respir. J. 46 (4) (2015) 976–987, https://doi.org/10.1183/13993003.00150-2015.

[2] B. Oehrle, G. Burgstaller, M. Irmler, et al., Validated prediction of pro-invasive growth factors using a transcriptome-wide invasion signature derived from a complex 3D invasion assay, Sci. Rep. 5 (5) (2015) 12673–12685, https://doi.org/10.1038/srep12673.

[3] K. Rydell-Tormanen, X.H. Zhou, O. Hallgren, et al., Aberrant nonfibrotic parenchyma in idiopathic pulmonary fibrosis is correlated with decreased beta-catenin inhibition and increased Wnt5a/b interaction, Phys. Rep. 4 (5) (2016) e12727–e12735, https://doi.org/10.14814/phy2.12727.

[4] P. Song, J.X. Zheng, J.Z. Liu, et al., Effect of the Wnt1/beta-catenin signalling pathway on human embryonic pulmonary fibroblasts, Mol. Med. Rep. 10 (2) (2014) 1030–1036, https://doi.org/10.3892/mmr.2014.2261.

[5] M. Tebar, O. Destree, W.J.A. de Vree, Ten have-Opbroek AAW. Expression of Tcf/Lef and sFrp and localization of beta-catenin in the developing mouse lung, Mech. Dev. 109 (2) (2001) 437–440.

[6] P. Dufourcq, L. Leroux, J. Ezan, et al., Regulation of endothelial cell cytoskeletal reorganization by a secreted frizzled-related protein-1 and frizzled 4- and frizzled 7-dependent pathway: role in neovessel formation, Am. J. Pathol. 172 (1) (2008) 37–49, https://doi.org/10.2353/ajpath.2008.070130.

[7] A. Akhmetshina, K. Palumbo, C. Dees, et al., Activation of canonical Wnt signalling is required for TGF-beta-mediated fibrosis, Nat. Commun. 13 (3) (2012) 735–737, https://doi.org/10.1038/ncomms1734.

[8] K.D. Salazar, S.M. Lankford, A.R. Brody, Mesenchymal stem cells produce Wnt isoforms and TGF-beta1 that mediate proliferation and procollagen expression by lung fibroblasts, Am. J. Physiol. Lung Cell. Mol. Physiol. 297 (5) (2009) L1002–L1011, https://doi.org/10.1152/ajplung.90347.2008.

[9] M. Konigshoff, N. Balsara, E.M. Pfaff, et al., Functional Wnt signaling is increased in idiopathic pulmonary fibrosis, PLoS One 3 (5) (2008) e2142–e2153, https://doi.org/10.1371/journal.pone.0002142.

[10] H.S. Melkonyan, W.C. Chang, J.P. Shapiro, et al., SARPs: a family of secreted apoptosis-related proteins, Proc. Natl. Acad. Sci. U. S. A. 94 (25) (1997) 13636–13641.

[11] Y. Kawano, R. Kypta, Secreted antagonists of the Wnt signalling pathway, J. Cell Sci. 116 (Pt 13) (2003) 2627–2634, https://doi.org/10.1242/jcs.00623.

[12] C. Dees, I. Schlottmann, R. Funke, et al., The Wnt antagonists DKK1 and SFRP1 are downregulated by promoter hypermethylation in systemic sclerosis, Ann. Rheum. Dis. 73 (6) (2014) 1232–1239, https://doi.org/10.1136/annrheumdis-2012-203194.

[13] P. Sklepkiewicz, T. Shiomi, R. Kaur, et al., Loss of secreted frizzled-related protein-1 leads to deterioration of cardiac function in mice and plays a role in human cardiomyopathy, Circ. Heart Fail. 8 (2) (2015) 362–372, https://doi.org/10.1161/CIRCHEARTFAILURE.114.001274.

[14] F. Hong, J. Hong, L. Wang, et al., Chronic exposure to nanoparticulate TiO_2 causes renal fibrosis involving activation of the Wnt pathway in mouse kidney, J. Agric. Food Chem. 63 (5) (2015) 1639–1647, https://doi.org/10.1021/jf5034834.

[15] R. Scardigli, C. Gargioli, D. Tosoni, et al., Binding of sFRP-3 to EGF in the extracellular space affects proliferation, differentiation and morphogenetic events regulated by the two molecules, PLoS One 3 (6) (2008) e2471–e2486, https://doi.org/10.1371/journal.pone.0002471.

[16] K. Matsushima, T. Suyama, C. Takenaka, et al., Secreted frizzled related protein 4 reduces fibrosis scar size and ameliorates cardiac function after ischemic injury, Tissue Eng. A 16 (11) (2010) 3329–3341, https://doi.org/10.1089/ten.TEA.2009.0739.

[17] D. Elhaj Mahmoud, N. Sassi, G. Drissi, et al., sFRP3 and DKK1 regulate fibroblast-like synoviocytes markers and Wnt elements expression depending on cellular context, Immunol. Investig. 46 (3) (2017) 314–328, https://doi.org/10.1080/08820139.2016.1267204.

[18] Z.Y. Zhang, A. Deb, Z.P. Zhang, et al., Secreted frizzled related protein 2 protects cells from apoptosis by blocking the effect of canonical Wnt3a, J. Mol. Cell. Cardiol. 46 (3) (2009) 370–377, https://doi.org/10.1016/j.yjmcc.2008.11.016.

[19] M. Li, Y. Zheng, H. Yuan, et al., Effects of dynamic changes in histone acetylation and deacetylase activity on pulmonary fibrosis, Int. Immunopharmacol. 52 (2017) 272–280, https://doi.org/10.1016/j.intimp.2017.09.020.

[20] Y.Y. Sanders, N. Ambalavanan, B. Halloran, et al., Altered DNA methylation profile in idiopathic pulmonary fibrosis, Am. J. Respir. Crit. Care Med. 186 (6) (2012) 525–535, https://doi.org/10.1164/rccm.201201-0077OC.

[21] E.I. Rabinovich, M.G. Kapetanaki, I. Steinfeld, et al., Global methylation patterns in idiopathic pulmonary fibrosis, PLoS One 7 (4) (2012) e33770–e33778, https://doi.org/10.1371/journal.pone.0033770.

[22] R.J. Klose, A.P. Bird, Genomic DNA methylation: the mark and its mediators, Trends Biochem. Sci. 31 (2) (2006) 89–97, https://doi.org/10.1016/j.tibs.2005.12.008.

[23] M. Karahoca, R.L. Momparler, Pharmacokinetic and pharmacodynamic analysis of 5-aza-2′-deoxycytidine (decitabine) in the design of its dose-schedule for cancer therapy, Clin. Epigenetics 5 (1) (2013) 3–18, https://doi.org/10.1186/1868-7083-5-3.

[24] P.A. Jones, S.M. Taylor, Cellular differentiation, cytidine analogs and DNA methylation, Cell 20 (1) (1980) 85–93.

[25] S.B. Russell, J.D. Russell, K.M. Trupin, et al., Epigenetically altered wound healing in keloid fibroblasts, J. Invest. Dermatol. 130 (10) (2010) 2489–2496, https://doi.org/10.1038/jid.2010.162.

[26] H.J. Yang, S.G. Kim, J.H. Lim, et al., Helicobacter pylori-induced modulation of the promoter methylation of Wnt antagonist genes in gastric carcinogenesis, Gastric Cancer 21 (2) (2018) 237–248, https://doi.org/10.1007/s10120-017-0741-6.

[27] J. Paluszczak, J. Sarbak, M. Kostrzewska-Poczekaj, et al., The negative regulators of Wnt pathway-DACH1, DKK1, and WIF1 are methylated in oral and oropharyngeal cancer and WIF1 methylation predicts shorter survival, Tumor Biol. 36 (4) (2015) 2855–2861, https://doi.org/10.1007/s13277-014-2913-x.

[28] Y. Liu, Y. Zheng, Bach1 siRNA attenuates bleomycin-induced pulmonary fibrosis by modulating oxidative stress in mice, Int. J. Mol. Med. 39 (1) (2017) 91–100, https://doi.org/10.3892/ijmm.2016.2823.

[29] B.L. Edelman, E.F. Redente, Isolation and characterization of mouse fibroblasts, Methods Mol. Biol. 2018 (1809) 59–67, https://doi.org/10.1007/978-1-4939-8570-8_5.

[30] C.J. Baglole, S.Y. Reddy, S.J. Pollock, et al., Isolation and phenotypic characterization of lung fibroblasts, Methods Mol. Med. 117 (2005) 115–127, https://doi.org/10.1385/1-59259-940-0:115.

[31] Q. Fu, Y. Zheng, X. Dong, et al., Activation of cannabinoid receptor type 2 by JWH133 alleviates bleomycin-induced pulmonary fibrosis in mice, Oncotarget 8 (61) (2017) 103486–103498, https://doi.org/10.18632/oncotarget.21975.

[32] A. Velroyen, A. Yaroshenko, D. Hahn, et al., Grating-based X-ray dark-field computed tomography of living mice, EBioMedicine 2 (10) (2015) 1500–1506, https://doi.org/10.1016/j.ebiom.2015.08.014.

[33] D. Lopera, T. Naranjo, J.M. Hidalgo, et al., Pulmonary abnormalities in mice with paracoccidioidomycosis: a sequential study comparing high resolution computed tomography and pathologic findings, PLoS Negl. Trop. Dis. 4 (6) (2010) e726–e734, https://doi.org/10.1371/journal.pntd.0000726.

[34] I.I. Rosen, T.A. Fischer, J.A. Antolak, et al., Correlation between lung fibrosis and radiation therapy dose after concurrent radiation therapy and chemotherapy for limited small cell lung cancer, Radiology 221 (3) (2001) 614–622, https://doi.org/10.1148/radiol.2213992043.

[35] S.V. Szapiel, N.A. Elson, J.D. Fulmer, et al., Bleomycin-induced interstitial pulmonary disease in the nude, athymic mouse, Am. Rev. Respir. Dis. 120 (4) (1979) 893–899, https://doi.org/10.1164/arrd.1979.120.4.893.

[36] T. Ashcroft, J.M. Simpson, V. Timbrell, Simple method of estimating severity of

pulmonary fibrosis on a numerical scale, J. Clin. Pathol. 41 (4) (1988) 467–470.
[37] T.D. Schmittgen, K.J. Livak, Analyzing real-time PCR data by the comparative C(T) method, Nat. Protoc. 3 (6) (2008) 1101–1108.
[38] H.A. Drury, P. Green, B.K. McCauley, et al., Spatial normalization of one-dimensional electrophoretic gel images, Genomics 8 (1) (1990) 119–126.
[39] A. Degasperi, M.R. Birtwistle, N. Volinsky, et al., Evaluating strategies to normalise biological replicates of Western blot data, PLoS One 9 (1) (2014) e87293–e87304, https://doi.org/10.1371/journal.pone.0087293.
[40] X.G. Li, P. Lu, B. Li, et al., Effects of iodine-125 seeds on the methylation of SFRP2 and P16 in colorectal cancer, Exp. Ther. Med. 6 (5) (2013) 1225–1228, https://doi.org/10.3892/etm.2013.1298.
[41] L. Liu, B. Carron, H.T. Yee, et al., Wnt pathway in pulmonary fibrosis in the bleomycin mouse model, J. Environ. Pathol. Toxicol. Oncol. 28 (2) (2009) 99–108.
[42] R. Foronjy, K. Imai, T. Shiomi, et al., The divergent roles of secreted frizzled related protein-1 (SFRP1) in lung morphogenesis and emphysema, Am. J. Pathol. 177 (2) (2010) 598–607, https://doi.org/10.2353/ajpath.2010.090803.
[43] J. Bai, Z. Liu, Z. Xu, et al., Epigenetic downregulation of SFRP4 contributes to epidermal hyperplasia in psoriasis, J. Immunol. 194 (9) (2015) 4185–4198.
[44] J. Bayle, J. Fitch, K. Jacobsen, et al., Increased expression of Wnt2 and SFRP4 in tsk mouse skin: role of Wnt signaling in altered dermal fibrillin deposition and systemic sclerosis, J. Invest. Dermatol. 128 (4) (2008) 871–881, https://doi.org/10.1038/sj.jid.5701101.
[45] L. Barandon, F. Casassus, L. Leroux, et al., Secreted frizzled-related protein-1 improves postinfarction scar formation through a modulation of inflammatory response, Arterioscler. Thromb. Vasc. Biol. 31 (11) (2011) E80–U60, https://doi.org/10.1161/ATVBAHA.111.232280.
[46] Y.O. Nunez Lopez, G. Garufi, M. Pasarica, et al., Elevated and correlated expressions of miR-24, miR-30d, miR-146a, and SFRP-4 in human abdominal adipose tissue play a role in adiposity and insulin resistance, Int. J. Endocrinol. 2018 (2018) 7351902–7351908, https://doi.org/10.1155/2018/7351902.
[47] I.V. Yang, B.S. Pedersen, E. Rabinovich, et al., Relationship of DNA methylation and gene expression in idiopathic pulmonary fibrosis, Am. J. Respir. Crit. Care Med. 190 (11) (2014) 1263–1272, https://doi.org/10.1164/rccm.201408-1452OC.
[48] S.K. Huang, A.M. Scruggs, R.C. McEachin, et al., Lung fibroblasts from patients with idiopathic pulmonary fibrosis exhibit genome-wide differences in DNA methylation compared to fibroblasts from nonfibrotic lung, PLoS One 9 (9) (2014) e107055–e107069, https://doi.org/10.1371/journal.pone.0107055.
[49] Y.Y. Sanders, A. Pardo, M. Selman, et al., Thy-1 promoter hypermethylation: a novel epigenetic pathogenic mechanism in pulmonary fibrosis, Am. J. Respir. Cell Mol. Biol. 39 (5) (2008) 610–618, https://doi.org/10.1165/rcmb.2007-0322OC.
[50] S.K. Huang, A.S. Fisher, A.M. Scruggs, et al., Hypermethylation of PTGER2 confers prostaglandin E2 resistance in fibrotic fibroblasts from humans and mice, Am. J. Pathol. 177 (5) (2010) 2245–2255, https://doi.org/10.2353/ajpath.2010.100446.
[51] J. Cisneros, J. Hagood, M. Checa, et al., Hypermethylation-mediated silencing of p14(ARF) in fibroblasts from idiopathic pulmonary fibrosis, Am. J. Physiol. Lung Cell. Mol. Physiol. 303 (4) (2012) L295–L303, https://doi.org/10.1152/ajplung.00332.2011.
[52] M.P. Ramos, N.A. Wijetunga, A.S. McLellan, et al., DNA demethylation by 5-aza-2′-deoxycytidine is imprinted, targeted to euchromatin, and has limited transcriptional consequences, Epigenetics Chromatin 8 (2015) 11–27, https://doi.org/10.1186/s13072-015-0004-x.
[53] E.A. Griffiths, S.D. Gore, DNA methyltransferase and histone deacetylase inhibitors in the treatment of myelodysplastic syndromes, Semin. Hematol. 45 (1) (2008) 23–30.
[54] Y.S. Kim, W.S. Kang, J.S. Kwon, et al., Protective role of 5-azacytidine on myocardial infarction is associated with modulation of macrophage phenotype and inhibition of fibrosis, J. Cell. Mol. Med. 18 (6) (2014) 1018–1027, https://doi.org/10.1111/jcmm.12248.
[55] R. Donate Puertas, E. Meugnier, C. Romestaing, et al., Atrial fibrillation is associated with hypermethylation in human left atrium, and treatment with decitabine reduces atrial tachyarrhythmias in spontaneously hypertensive rats, Transl. Res. 184 (2017) 57–67, https://doi.org/10.1016/j.trsl.2017.03.004.
[56] S. Pushpakumar, S. Kundu, N. Narayanan, et al., DNA hypermethylation in hyperhomocysteinemia contributes to abnormal extracellular matrix metabolism in the kidney, The FASEB Journal 29 (11) (2015) 4713–4725, https://doi.org/10.1096/fj.15-272443.
[57] B.A. Vervaet, L. Moonen, L. Godderis, et al., Untargeted DNA-demethylation therapy neither prevents nor attenuates ischemia-reperfusion-induced renal fibrosis, Nephron 137 (2) (2017) 124–136, https://doi.org/10.1159/000477507.